Intravenous insulin administration preparation for myocardial ^{18}F-fluorodeoxyglucose viability imaging has the potential to reduce radiation exposure dose

Yangchun Chen (fudanzhsh@ymail.com)
Fujian Medical University Affiliated First Quanzhou Hospital https://orcid.org/0000-0002-9076-6581
Qingqing Wang
Fujian Medical University Affiliated First Quanzhou Hospital
Peihao Huang
Fujian Medical University Affiliated First Quanzhou Hospital
Yuehui Wang
Fujian Medical University Affiliated First Quanzhou Hospital
Yuxuan Chen
Fujian Medical University Affiliated First Quanzhou Hospital
Huilin Zhuo
Fujian Medical University Affiliated First Quanzhou Hospital
Ruozhu Dai
Fujian Medical University Affiliated First Quanzhou Hospital
Huoqiang Wang
Tongji University Affiliated Shanghai Pulmonary Hospital

Original research

Keywords: insulin, 18F-fluorodeoxyglucose, radiation dose, equivalence trial

Posted Date: September 21st, 2021

DOI: https://doi.org/10.21203/rs.3.rs-791504/v2

Abstract

Purpose

This study aimed to identify and validate the optimal ^{18}F-FDG activity and acquisition time for cardiac viability imaging with intravenous insulin administration based on a fixed ^{18}F-FDG activity.

Methods

Cardiac positron emission tomography (PET) images from 30 patients with coronary artery disease (CAD) were retrospectively reconstructed into 900, 360, 180, 90, and 45 s durations. An optimal product of the maximum standardized uptake value (SUV) of the myocardium and segmental uptake (SU) and acquisition time (MSAT) was determined through a receiver operating characteristic curve. The optimal acquisition time (OAT) was equal to MSAT divided by mean SUV of the myocardium (MyoSUV) and validated in another 26 patients with CAD.

Results

The MyoSUV, mean SUV of the blood, SU, and their biases on reconstructed image durations of 90, 180, and 360 s were equivalent to those on an image duration of 900 s. The optimal MSAT was 848.2. In the validation group, the OAT was 129 ± 76 s (95% confidence interval, 99–160), approximately one-third of the usual acquisition time. The MyoSUV and SU were equivalent for the difference (0.15 ± 0.21, $P < 0.001$; −0.01 ± 0.03, $P < 0.001$) between PET image duration of OAT and 600 s (7.71 ± 3.01 vs. 7.56 ± 2.94, 67.1 ± 15.4% vs. 67.7 ± 15.6%).

Conclusion

Intravenous insulin administration preparation has the potential to reduce radiation exposure and acquisition time of cardiac ^{18}F-FDG viability imaging without losing the accurate measurement of MyoSUV and SU when reaching an OAT.

Introduction

High signal-to-noise ratio is a critical factor for a precise positron emission tomography (PET) quantitative analysis. The signal-to-noise ratio of PET image improvement depends on the new crystals [1, 2], new reconstruction methods [3–5], time-of-flight application [6, 7], axial field of view expansion [8], and use of magnetic resonance [9] and ultrasound [10] equipment. In clinical practice, optimizing acquisition time [11], increasing tracer dosage [12], and enhancing the tracer uptake ability of the organ of interest improve PET image quality. Insulin enhances myocardial glucose uptake by stimulating

glucose transporter 4 onto the cardiomyocyte membrane [13] and surpasses the standardized glucose loading preparation protocol for myocardial viability ^{18}F-fluorodeoxyglucose (^{18}F-FDG) imaging [14]. Therefore, insulin has the potential to obtain high-quality cardiac ^{18}F-FDG images with decreasing ^{18}F-FDG activity to reduce radiation dose.

Counts in the myocardium are lower with greater variability of segmental ^{18}F-FDG uptake in low-dose ^{18}F-FDG imaging compared to normal-dose imaging. However, coronary artery revascularization in severe left ventricular dysfunction is based on precise myocardial ^{18}F-FDG uptake analysis [15, 16]. ^{18}F-FDG activity is positively associated with the radiation dose and the PET image count, whereas the count variation is negatively associated with the PET image count. Measurement error is greater with smaller counts; therefore, precise analysis is needed to avoid high doses of radiation caused by high ^{18}F-FDG activity. The optimal ^{18}F-FDG activity for cardiac viability imaging remains unknown. Since the product of ^{18}F-FDG activity and scan duration per bed position (MBq/kg × min/bed) is a critical factor for optimizing PET data acquisition, the ^{18}F-FDG activity is inversely proportional to the scan duration [17]. Therefore, this study aimed to validate, following the determination of the optimal ^{18}F-FDG activity, the optimal acquisition time (OAT) for cardiac viability ^{18}F-FDG imaging based on a fixed ^{18}F-FDG activity.

Materials And Methods

Participants

In this retrospective study, a total of 30 patients with coronary artery disease were included from our registered trial (ChiCTR1800019741) to develop an OAT for cardiac viability ^{18}F-FDG imaging. Another group of patients with coronary artery disease for cardiac viability ^{18}F-FDG imaging was randomly selected from our database and approved by the ethics committee of our hospital (registration number 106). All patients signed an informed consent form before imaging with insulin loading preparation. The patients fasted ≥ 6 h before blood glucose measurement. In the development group, routine intravenous insulin (dosage (IU) = blood glucose (mmol/L) − 2) was administered approximately 24 min before ^{18}F-FDG injection with a 10% incremental dose for diabetic patients [14]. In the validation group, intravenous regular insulin (dosage (IU) = k × [blood glucose (mmol/L) − 2] × weight (kg); where k = 0.02 and 0.023 for non-diabetic and diabetic patients, respectively) was administered approximately 20 min before ^{18}F-FDG injection with or without 250 mL of whole milk [18].

Cardiac ^{18}F-fluorodeoxyglucose positron emission tomography/computed tomography data acquisition and reconstruction

Cardiac PET data were acquired with a three-dimensional list mode, 200 × 200 matrix, using PET/computed tomography (Biograph mCT Flow64, Siemens, Malvern, PA, USA) with 15 and 10 min/bed approximately 90 and 50 min after ^{18}F-FDG (3.7 MBq/kg) injection in the development and validation

group, respectively. Attenuation-corrected cardiac PET images were retrospectively reconstructed with iterative TrueX (Siemens, Malvern, PA, USA; 3 iterations, 24 subsets) into 900, 360, 180, 90, and 45 s durations in the development group, although they were retrospectively reconstructed into 30 and 600 s and optimal acquisition duration in the validation group.

Qualitative and quantitative image analyses

Standardized uptake value (SUV) measurements were performed with TrueD (Siemens, Malvern, PA, USA). A volume of interest with approximately 1.6 cm diameter was placed in the right atrium to measure the mean SUV of the blood (BloSUV). Moreover, 41% maximal myocardial SUV (MyoSUVmax) was set as the cutoff value to measure the mean SUV of the myocardium (MyoSUV) [17]. Segmental uptake (SU) percent was automatically analyzed using the quantitative perfusion single-photon emission computed tomography 2012 version (Cedars-Sinai Medical Center, Los Angeles, CA, USA) and displayed on a 17-segment polar map. SUVs and SU from 900 and 600 s image durations were set as true values in the development and validation groups, respectively. Bias of SUV and SU describes the relative percentage difference of their estimated values from true values. Bias within ±0.10 was acceptable [19]. The OAT was defined to obtain more than 16/17 segments with biases within 0.10 of the minimum acquisition time.

Statistical analyses

Continuous variables are expressed as mean ± standard deviation. Categorical variables are expressed as percentages. Between-group comparisons were performed using equivalence paired *t*-tests and chi-squared tests as appropriate. The equivalent limitation values of the SUV of the blood pool and myocardium were set as ± 0.1 and ± 0.5, respectively. The power and significance were set at 90% and 5%, respectively. Because biases of SU were affected by counts in the volume of interest, the product of MyoSUVmax and SU and acquisition time (MSAT) was set as the independent variable. A receiver operating characteristic curve analysis was performed, and the cutoff value of MSAT was determined, with a specificity ≥ 16/17.

In the validation group, the sample size was calculated according to the bias of MyoSUV obtained from a 90-s image duration in the development group. The OAT was calculated as MSAT divided by MyoSUV obtained from a 30-s image duration. The SUV and SU of the left ventricular myocardium on the image reconstructed with optimal time were compared with those on images acquired at 600 s.

Results

The quantitative parameters in the development group are listed in TABLE 1. The MyoSUV, BloSUV, SU, and their biases on reconstructed image durations of 90, 180, and 360 s were equivalent to their true

values. However, biases of SUVs and SU increased as duration time decreased. The MyoSUV, MyoSUVmax, and BloSUVmax on reconstructed 45 s image durations were not equivalent to their true values.

The area under the receiver operating characteristic curve was 0.833 ± 0.018 (95% confidence interval [CI], 0.798–0.869; P < 0.001). When MSAT was > 848.2, the ratio of bias of SU beyond ± 0.10 was ≤ 5.3%; in other words, the ratio of SU within ± 0.10 was ≥ 16/17 segments (FIG 1).

A total of 26 patients were required in the validation group to obtain significant results. The baseline characteristics of patients in the validation group were similar to those of the development group (TABLE 2). In the validation group, the MyoSUV was 7.94 ± 3.02 on the PET 30 s image duration. The OAT was 129 ± 76 s (95% CI, 99–160). The MyoSUV was equivalent for the difference (0.15 ± 0.21, P < 0.001) between the PET OAT image duration and 600 s image duration (7.71 ± 3.01 vs. 7.56 ± 2.94). The SU was equivalent for the difference (–0.01 ± 0.03, P<0.001) between cardiac OAT image duration and 600 s image duration (67.1 ± 15.4% vs. 67.7 ± 15.6%). A patient with severe heart failure with left anterior descending artery and left circumflex artery chronic total occlusion underwent ^{18}F-FDG viability imaging before revascularization. The MyoSUV measured on his myocardial PET images reconstructed into 30 s duration was 7.0. His OAT was equal to 121 s. Subsequently, his myocardial PET images were reconstructed into 121 and 600 s duration and automatically analyzed with quantitative perfusion single-photon emission computed tomography and are shown in FIGURE 2. Biases of MyoSUV and SU in each segment were within 0.1 on 121 s image duration.

Discussion

The concept of cardiac ^{18}F-FDG viability imaging with insulin loading preparation, acquired with optimal time was established and confirmed for the first time in this study. Our results are robust. The optimization acquisition time was determined through objective analysis instead of subjectivity adjustment [8, 20] and it was confirmed in another similar validation group. The MyoSUV and SU were significantly equivalent between cardiac OAT image duration and 600-s image duration (P < 0.001). The OAT was only approximately one-third of the usual acquisition time (360 s) with a fixed ^{18}F-FDG dose (3.7 MBq/kg). This suggests that only one-third of the radiation dose exposure to ^{18}F-FDG may be achieved when the ^{18}F-FDG dose is reduced to 1.2 MBq/kg with usual acquisition time (360 s). Because the effective dose of ^{18}F-FDG for adults is 0.019 mSv/MBq [21], the average effective radiation dose is only 1.6 mSv for a 70-kg patient.

SU in 17 segments is a semiquantitative assessment of myocardial ^{18}F-FDG viability [22]. It is more precise than MyoSUV. Because SUs obtained from quantitative perfusion single-photon emission computed tomography are equivalent between cardiac OAT and 600-s image durations, it implies that the efficiency of cardiac viability assessment based on ^{18}F-FDG image acquisition duration OAT is similar to that of 600 s acquisition duration.

Because the variation of MyoSUV is large (> 30%), an empirical OAT is difficult to determine. However, a pragmatic self-adapting acquisition mode can solve that problem. The OAT can be calculated according to the MyoSUV obtained from a prior acquiring cardiac data (30-s duration). Moreover, the data acquisition will continue to trigger the OAT. This type of simulating acquisition mode has been confirmed in the validation group. We believe that this type of pragmatic self-adapting acquisition mode would be produced in the future.

Limitations

There are two limitations in this study. First, the MSAT was determined from cardiac data acquisition with a three-dimensional mode using PET/computed tomography and only adapted this condition. Because detection sensitivity and noise equivalent count rates vary among commercial PET scanners [23, 24], even acquisition modes (two-dimensional/three-dimensional) in the same gantry [25], as well as MSAT values, may differ and must be determined under each condition. Second, cardiac motions were non-corrected for myocardial PET images in this study. Because the signal-to-noise ratio increases with cardiac motion correction for myocardial PET images [26], the MSAT could decrease with motion correction, which may cause a shorter OAT and a lower radiation exposure dose.

Conclusion

Intravenous insulin administration preparation has the potential to reduce radiation exposure and acquisition time of cardiac ^{18}F-FDG viability imaging without losing the accurate measurement of MyoSUV or SU percent when reaching an OAT.

Declarations

Ethics approval and consent to participate

This retrospective study involving human participants was in accordance with the ethical standards of the institutional and national research committee and with the 1964 Helsinki Declaration and its later amendments or comparable ethical standards. The ethics committee of Quanzhou 1st hospital approved this study. All patients signed an informed consent form before imaging with insulin loading preparation.

Consent for publication

Not applicable.

Availability of data and material

The datasets generated and analysed during the current study are not publicly available due to participant privacy but are available from the corresponding author on reasonable request.

Competing interests

The authors declare that they have no competing interests.

Funding

The trial was supported by the Natural Science Foundation of Fujian Province (Grant numbers 2015J01516, 2018J01202, 2020J011280), and the Quanzhou Science and Technology Commission (Grant number 2019C023R).

Authors' contributions

Yangchun Chen and Ruozhu Dai received various funding and supervised this study. Yangchun Chen designed this study, and Huoqiang Wang modified that designation. Qingqing Wang, Peihao Huang, Yuehui Wang, Yuxuan Chen, Huilin Zhuo, and Yangchun Chen conducted this study. Yangchun Chen wrote the draft manuscript. We have read, revised that draft and approved the final version of this manuscript.

Acknowledgements

Not applicable.

References

1. van Sluis J, Boellaard R, Dierckx RAJO, Stormezand GN, Glaudemans AWJM, Noordzij W. Image Quality and Activity Optimization in Oncologic ^{18}F-FDG PET Using the Digital Biograph Vision PET/CT System. J Nucl Med. 2020;61:764–71.
2. van Sluis J, Boellaard R, Somasundaram A, et al. Image Quality and Semiquantitative Measurements on the Biograph Vision PET/CT System: Initial Experiences and Comparison with the Biograph mCT. J Nucl Med. 2020;61:129–35.
3. Arabi H, Zaidi H. Improvement of image quality in PET using post-reconstruction hybrid spatial-frequency domain filtering. Phys Med Biol. 2018;63:215010.
4. Cui J, Gong K, Guo N, et al. PET image denoising using unsupervised deep learning. Eur J Nucl Med Mol Imaging. 2019;46:2780–9.
5. Song TA, Chowdhury SR, Yang F, Dutta J. PET image super-resolution using generative adversarial networks. Neural Netw. 2020;125:83–91.
6. Zhang Z, Rose S, Ye J, et al. Optimization-Based Image Reconstruction From Low-Count, List-Mode TOF-PET Data. IEEE Trans Biomed Eng. 2018;65:936–46.
7. Armstrong IS, Tonge CM, Arumugam P. Assessing time-of-flight signal-to-noise ratio gains within the myocardium and subsequent reductions in administered activity in cardiac PET studies. J Nucl Cardiol. 2019;26:405–12.
8. Zhang YQ, Hu PC, Wu RZ, et al. The image quality, lesion detectability, and acquisition time of 18F-FDG total-body PET/CT in oncological patients. Eur J Nucl Med Mol Imaging. 2020;47:2507–15.

9. Munoz C, Kunze KP, Neji R, et al. Motion-corrected whole-heart PET-MR for the simultaneous visualisation of coronary artery integrity and myocardial viability: an initial clinical validation. Eur J Nucl Med Mol Imaging. 2018;45:1975–86.
10. Perez-Liva M, Yoganathan T, Herraiz JL, et al. Ultrafast Ultrasound Imaging for Super-Resolution Preclinical Cardiac PET. Mol Imaging Biol. 2020;22:1342–52.
11. Murthy V, Smith RL, Tao DH, et al. 68Ga-PSMA-11 PET/MRI: determining ideal acquisition times to reduce noise and increase image quality. EJNMMI Phys. 2020;7:54.
12. Cox CPW, Segbers M, Graven LH, Brabander T, van Assema DME. Standardized image quality for 68Ga-DOTA-TATE PET/CT. EJNMMI Res. 2020;10:27.
13. Jaldin-Fincati JR, Pavarotti M, Frendo-Cumbo S, Bilan PJ, Klip A. Update on GLUT4 Vesicle Traffic: A Cornerstone of Insulin Action. Trends Endocrinol Metab. 2017;28:597–611.
14. Chen YC, Wang QQ, Wang YH, Zhuo HL, Dai RZ. Intravenous regular insulin is an efficient and safe procedure for obtaining high-quality cardiac 18F-FDG PET images: an open-label, single-center, randomized controlled prospective trial. J Nucl Cardiol. 2020 Jun 12.[Epub ahead of print].
15. Chareonthaitawee P, Gersh BJ, Araoz PA, Gibbons RJ. Revascularization in severe left ventricular dysfunction: the role of viability testing. J Am Coll Cardiol. 2005;46:567–74.
16. Moody JB, Hiller KM, Lee BC, et al. The utility of 82Rb PET for myocardial viability assessment: Comparison with perfusion-metabolism 82Rb-18F-FDG PET. J Nucl Cardiol. 2019;26:374–86.
17. Boellaard R, Delgado-Bolton R, Oyen WJ, et al. FDG PET/CT: EANM procedure guidelines for tumour imaging: version 2.0. Eur J Nucl Med Mol Imaging. 2015;42:328–54.
18. Chen YC, Pan MJ, Wang QQ, Wang YH, Zhuo HL, Dai RZ. Intravenous insulin injection supplemented with subsequent milk consumption is a safer formulation for cardiac viability 18F-FDG imaging. J Nucl Cardiol 2021 May 5. [Epub ahead of print].
19. Scheuermann JS, Saffer JR, Karp JS, Levering AM, Siegel BA. Qualification of PET scanners for use in multicenter cancer clinical trials: the American College of Radiology Imaging Network experience. J Nucl Med. 2009;50:1187–93.
20. Zhao YM, Li YH, Chen T, et al. Image quality and lesion detectability in low-dose pediatric (18)F-FDG scans using total-body PET/CT. Eur J Nucl Med Mol Imaging 2021.
21. Dorbala S, Di Carli MF, Delbeke D, et al. SNMMI/ASNC/SCCT guideline for cardiac SPECT/CT and PET/CT 1.0. J Nucl Med. 2013;54:1485–507.
22. Lehner S, Uebleis C, Schüßler F, et al. The amount of viable and dyssynchronous myocardium is associated with response to cardiac resynchronization therapy: initial clinical results using multiparametric ECG-gated [18F]FDG PET. Eur J Nucl Med Mol Imaging. 2013;40:1876–83.
23. Doot RK, Scheuermann JS, Christian PE, Karp JS, Kinahan PE. Instrumentation factors affecting variance and bias of quantifying tracer uptake with PET/CT. Med Phys. 2010;37:6035–46.
24. Boellaard R, Rausch I, Beyer T, et al. Quality control for quantitative multicenter whole-body PET/MR studies: A NEMA image quality phantom study with three current PET/MR systems. Med Phys.

2015;42:5961–9.

25. van der Weerdt AP, Boellaard R, Visser FC, Lammertsma AA. Accuracy of 3D acquisition mode for myocardial FDG PET studies using a BGO-based scanner. Eur J Nucl Med Mol Imaging. 2007;34:1439–46.
26. Marchesseau S, Totman JJ, Fadil H, et al. Cardiac motion and spillover correction for quantitative PET imaging using dynamic MRI. Med Phys. 2019;46:726–37.

Tables

TABLE 1. Standardized uptake values of the blood pool and left ventricular myocardium, segmental ^{18}F-FDG uptake percent and their biases in the development group

Time(s)	45	90	180	360	900
BloSUVmax	1.57 ± 0.44	1.49 ± 0.46	1.44 ± 0.43	1.38 ± 0.44*	1.35 ± 0.42
BloSUV	1.05 ± 0.32*	1.05 ± 0.33*	1.04 ± 0.33*	1.02 ± 0.32*	1.00 ± 0.33
Bias of BloSUV	0.06 ± 0.08	0.05 ± 0.06*	0.04 ± 0.05*	0.02 ± 0.04*	
MyoSUVmax	10.92 ± 4.44	10.67 ± 4.28*	10.62 ± 4.31*	10.48 ± 4.23*	10.40 ± 4.20
MyoSUV	6.35 ± 2.66	6.25 ± 2.61*	6.22 ± 2.61*	6.17 ± 2.57*	6.06 ± 2.59
Bias of MyoSUV	0.04 ± 0.05*	0.02 ± 0.04*	0.02 ± 0.03*	0.01 ± 0.02*	
SU (%)	61.7 ± 15.8*	62.3 ± 15.5*	62.8 ± 15.6*	63.0 ± 15.8*	62.8 ± 15.8
Bias of SU	-0.02 ± 0.07*	-0.01 ± 0.05*	0.00 ± 0.04*	0.00 ± 0.03*	

Note: *P<0.05

BloSUVmax, maximum BloSUV; SUV, standardized uptake value; BloSUV, SUV of blood; MyoSUVmax, maximum MyoSUV; MyoSUV, SUV of myocardium; SU, segmental uptake

TABLE 2. The characteristics of patients in the development and validation groups

	Development group (n = 30)	Validation group (n=26)	p
Age--yr	61.4 ± 12.0	61.5 ± 12.8	0.90
Female--no.(%)	3 (10.0%)	5(19.2%)	0.45
Diabetes--no.(%)	10 (33.3%)	7(26.9%)	0.60
Previous MI--no.(%)	8 (26.7%)	6(23.1%)	0.76
Weight--kg	66.7 ± 12.7	63.1 ± 10.2	0.80
Height--cm	165.9 ± 6.9	165.9 ± 6.5	0.90
BMI--kg/m^2	24.2 ± 3.7	22.9 ± 3.5	0.76

MI, myocardial infarction; BMI, body mass index

TABLE 3. Standardized uptake values of the blood pool and left ventricular myocardium and their biases in the validation group

Time(s)	30	Optimization	600
BloSUVmax	1.74 ± 0.54	1.47 ± 0.51	1.40 ± 0.49
BloSUV	1.05 ± 0.39	1.02 ± 0.39	0.99 ± 0.37
Bias of BloSUV	0.07 ± 0.11	0.04 ± 0.12	
MyoSUVmax	13.54 ± 4.87	12.86 ± 4.79	12.48 ± 4.52
MyoSUV	7.94 ± 3.02	7.71 ± 3.01*	7.56 ± 2.94
Bias of MyoSUV		0.02 ± 0.03*	

Note: *P<0.05

BloSUVmax, maximum BloSUV; SUV, standardized uptake value; BloSUV, SUV of blood; MyoSUVmax, maximum SUV of myocardium; MyoSUV, SUV of myocardium

Figures

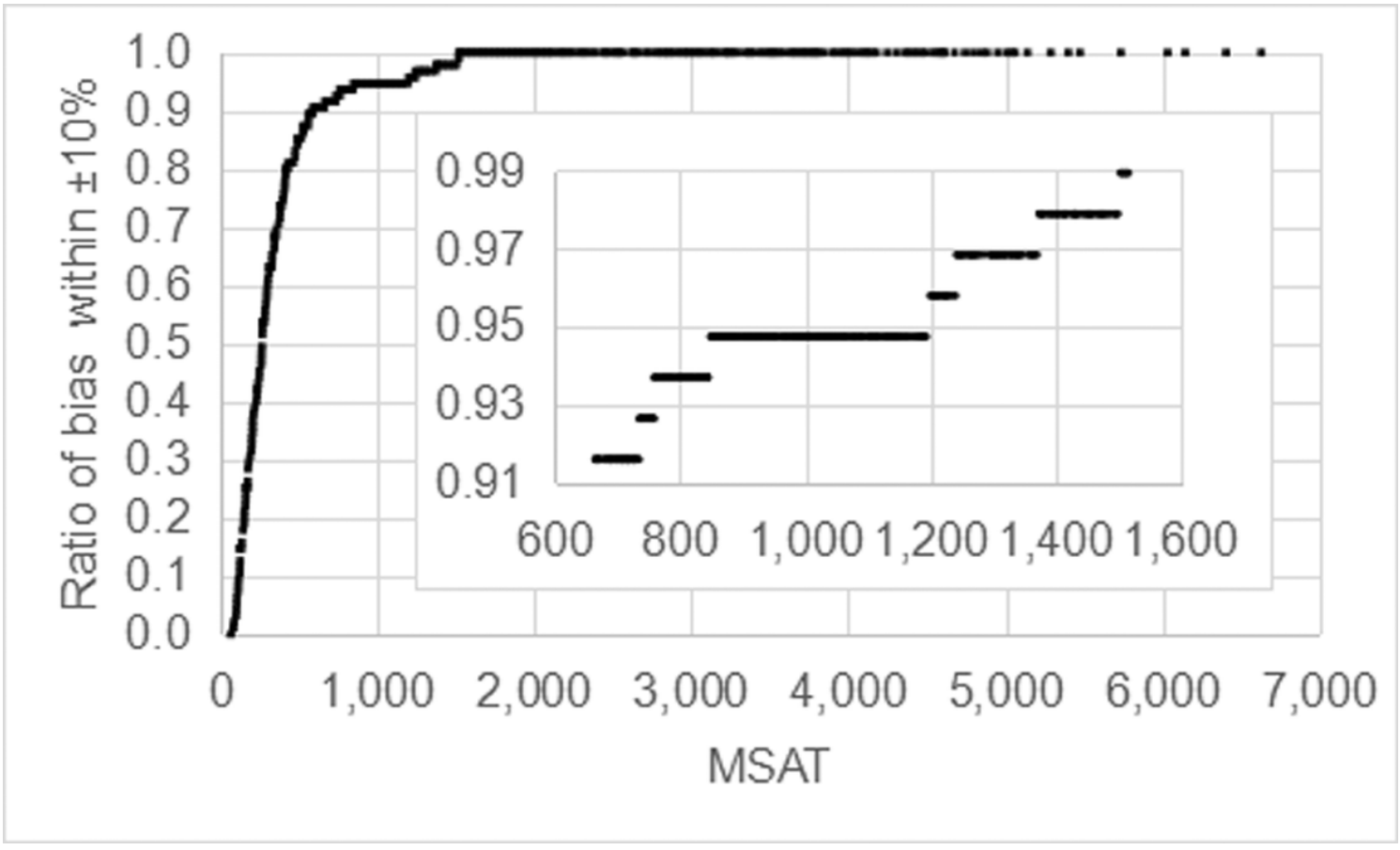

Figure 1

The association between the product of maximal myocardial standardized uptake value and segmental uptake and acquisition time (MSAT) and the ratio of bias of segmental uptake within ±10%.

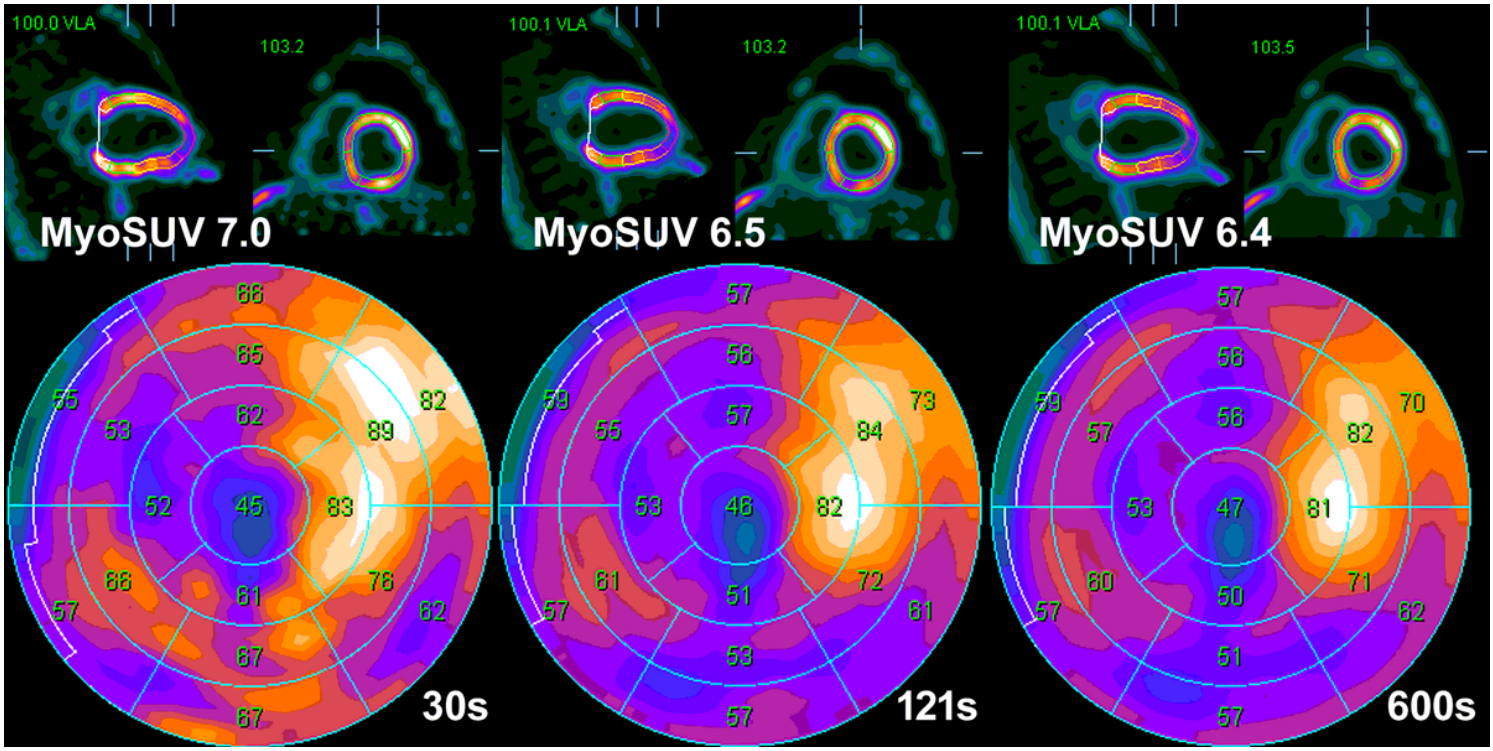

Figure 2

A series of representative myocardial 18F-fluorodeoxyglucose viability images reconstructed in 30, 121, and 600 s durations is shown as short axial, vertical long axial, and polar map images. The mean standardized uptake value of the myocardium (MyoSUV) on the prior positron emission tomography (PET) 30 s acquisition duration is 7.0. The MyoSUV and segmental uptake in each segment are equivalent (bias < ±0.05) on PET images reconstructed between 121 and 600 s duration.